

S.V. Kim<sup>\*1, 2</sup>, M.I. Baikenov<sup>1</sup>, K.S. Ibishev<sup>2</sup>,  
M.G. Meiramov<sup>3</sup>, Fengyun Ma<sup>4</sup>, T.O. Khamitova<sup>5</sup>

<sup>1</sup>Karagandy University of the name of academician E.A. Buketov, Karaganda, Kazakhstan;

<sup>2</sup>Zh. Abishev Chemical and Metallurgical Institute, Karaganda, Kazakhstan;

<sup>3</sup>Institute of Organic Synthesis and Coal Chemistry, Karaganda, Kazakhstan;

<sup>4</sup>Xinjiang University, Xinjiang, China;

<sup>5</sup>S. Seifullin Kazakh Agro Technical University, Nur-Sultan, Kazakhstan

(\*Corresponding author's e-mail: [vanquishV8@mail.ru](mailto:vanquishV8@mail.ru))

## Effect of Nickel Nanopowder on the Thermal Degradation of Coal Tar Distillate

Regularities of influence of nickel nanopowder on the thermal degradation of coal tar distillate were determined using model-free Kissinger, Flynn-Wall-Ozawa and model-fitting Coats-Redfern methods. Coal tar distillate with a boiling point of <350 °C was obtained by simple distillation of primary coal tar from the Shubarkol deposit. Nickel nanopowder was used as a catalyst and was added to coal tar distillate in a quantity of 1 % of the mass of the distillate and then the process of thermal degradation of coal tar distillate was conducted at heating rates 5, 10 and 20 °C/min in an inert gas medium. Nickel powder was obtained by high-voltage discharge impact on the dc electrolysis. X-ray diffraction (XRD) analysis showed that the obtained nickel powder has face-centered cubic structure and the average crystallite size calculated by the Scherrer equation was ~ 34 nm. Calculations of activation energy were performed via processing of thermogravimetric data. The Kissinger method showed that the activation energy value decreases from 145.19 kJ/mol to 43.65 kJ/mol, by the Flynn-Wall-Ozawa (FWO) method the value decreases from 152.82 kJ/mol to 51.65 kJ/mol, and by the Coats-Redfern method the value decreases from 143.38 kJ/mol to 52.64 kJ/mol. Applicability of these methods is ensured by the high values of correlation coefficients.

**Keywords:** thermal degradation, nickel, nanopowder, coal tar, distillate, crystallite, thermogravimetric analysis, activation energy.

### Introduction

The increasing demands placed on the quality of technological processing of organic raw materials [1] are primarily related to more stringent environmental requirements [2], point to the need for in-depth research on the development of methods for obtaining effective catalytic systems [3]. Studies on the development and application of various nanoheterogeneous catalytic systems for the processing of organic raw materials have risen in recent decades [4]. Nickel and its compounds are widely used in the production of various catalytic systems. The processes of aquathermolysis in the presence of iron, cobalt, and nickel at 300 °C improve the quality of heavy oil increasing the amount of low-molecular alkanes and reducing content of resins, asphaltenes, polyaromatic compounds, sulfur and nitrogen [5]. For instance, it was found that the pumping hydrogen, nickel-molybdenum nanoparticles in the form of a suspension in a vacuum oil residue at 360 °C in carbonate reservoirs was leading to destruction of almost 50 % of asphaltenes thus causing heavy oil liquefaction and increasing oil recovery [6].

Palladium-nickel phosphide deposited on a silicone-aluminum phosphate molecular sieve contributes to a more orderly mechanism of hydroisomerization of *n*-hexadecane, which leads to a high yield of isomerization products [7].

Coal tar can serve as a raw material for producing gasoline, diesel fuel, etc. For example, the simultaneous use of NiW/γ-Al<sub>2</sub>O<sub>3</sub> and NiW/SAPO-11 catalysts in the process of hydrotreating low-temperature resin in a two-stage reactor makes it possible to obtain jet fuel with a freezing point of -51 °C and a high heat value [8]. The catalytic hydrogenation of coal tar in a reactor with two fixed layers in the presence of two catalysts MoNi/γ-Al<sub>2</sub>O<sub>3</sub> and of WNiP/γ-Al<sub>2</sub>O<sub>3</sub>-USY leads to formation of diesel and gasoline fractions with a reduced sulfur and nitrogen content [9]. The Ni/ZSM-5 catalyst obtained by decomposition of nickel tetracarbonyl promotes to deeper hydrogenation of low-temperature and high-temperature resins, and also contributes to the removal of sulfur and nitrogen [10].

Hydrogenation of a mixture of resin and oil distillation residue with the addition of nickel nitrate and elemental sulfur leads to formation of products which are suitable for coke producing with a more ordered structure and yield greater than with the use of industrial catalysts [11].

Mesoporous spherical NiO-containing catalyst promotes the complete decomposition of anthracene in the hydrogenation process at 300 °C [12]. High conversion of anthracene was observed when hydrogenation process of anthracene in the presence of NiCo supported on chrysotile [13].

NiO supported on chrysotile leads to a significant reduction of activation energy in the process of thermal destruction of primary coal tar/polymeric materials mixture [14].

In this work, the kinetics of thermal degradation of primary coal tar distillate from the Shubarkol deposit without a catalyst and with the addition of nickel nanopowder in a quantity of 1 % of the mass of the organic compound was studied. Nickel nanopowder obtained by the action of a high-voltage discharge on the electrolysis process was used as a catalyst [15].

### *Experimental*

The composition of coal tar distillate obtained by simple distillation of primary coal tar to 350 °C was determined using an Agilent 7890A gas chromatograph having an Agilent 5975C mass-selective detector. Column parameters Rxi-5ms: length — 30 m, diameter — 0.25 mm, column adsorbent thickness — 0.25 microns, column heating rate 8 °C/min, carrier gas — helium; gas pressure in the column  $1.38 \times 10^5$  Pa; sample volume  $2 \times 10^{-4}$  cm<sup>3</sup>; input mode — split, library — NIST08. The composition of fractions was determined by a semi-quantitative method relative to the peak area. Data processing was carried out using the GS-MSD Data Analysis program.

The surface morphology of the nickel powder was studied using the MIRA 3 TESCAN scanning electron microscope (SEM). Phase composition and crystallite size of nickel powder were determined using X-ray diffraction (XRD) analysis and energy dispersion spectroscopy (EDS). X-ray diffraction analysis was performed on Shimadzu XRD-6000 diffractometer with CuK $\alpha$ -radiation with a wavelength  $\lambda = 0.15418$  nm. Phase identification was carried out using PDF 4+ databases, as well as the POWDER CELL 2.4 full-profile analysis program.

The average crystallite size of nickel powder was calculated for the largest diffraction peak (111), using the Scherrer equation for spherical particles of cubic symmetry:

$$D = \frac{0.94 \cdot \lambda}{B \cdot \cos \theta}, \quad (1)$$

where  $D$  — the average crystallite size (nm);  $\lambda$  — the X-ray diffractometer wavelength (nm);  $B$  — the line broadening at half the maximum intensity (radians);  $\theta$  — the Bragg angle. In this equation  $K$  — the numerical factor dependent on crystallite shape and in our case  $K = 0.94$ .

Thermogravimetric analysis was performed on the Labsys Evo TG-DTA/DSC 1600 °C derivatograph (Setaram, France) at heating rates of 5, 10 and 20 °C/min, in nitrogen atmosphere.

Since the distillate is a liquid organic mass, it was mixed with Al<sub>2</sub>O<sub>3</sub> to avoid boiling and splashing. Al<sub>2</sub>O<sub>3</sub> was pre-calcined at 600 °C for 4 hours. Distillate with the mass of 5 g was mixed with Al<sub>2</sub>O<sub>3</sub> in the ratio of 1:4.

Sample containing nickel powder was prepared as follows: 5 g of the distillate was mixed with the 0.05 g (1 % of distillate weight) nickel powder and this mixture was thoroughly stirred. Then Al<sub>2</sub>O<sub>3</sub> was added to obtained mixture with the same ratio as in the case of sample without nickel powder.  $10 \cdot 10^{-3}$  g of obtained mixture was taken for thermal analysis.

The kinetic parameters were determined based on the assumptions that the rate of transformation of a substance is a linear function depending on the temperature  $T$  and conversion  $\omega$  [16]:

$$\frac{d\omega}{dt} = k(T) f(\omega), \quad (2)$$

where  $\omega$  — the conversion which can be found from the relation [17, 18]:

$$\omega = \frac{m_i - m_t}{m_i - m_e}, \quad (3)$$

where  $m_i$  — the initial mass sample;  $m_t$  — the mass at time;  $m_e$  — the final mass.

The basic equation for non-isothermal conditions has the form:

$$\frac{d\omega}{dt} = \frac{Z}{\beta} \exp\left(-\frac{E}{RT}\right) f(\omega), \quad (4)$$

where  $Z$  — the pre-exponential or frequency factor ( $\text{sec}^{-1}$ );  $R = 8.314 \text{ kJ}/(\text{mol}\cdot\text{K})$  — the universal gas constant;  $T$  — the temperature (K);  $E$  — the activation energy (kJ/mol);  $\beta$  — the heating rate.

The Kissinger and Flynn-Wall-Ozawa model-free methods and the Coats-Redfern model method were used to evaluate the effect of nanosized nickel powder on changing the activation energy.

The calculation of kinetic parameters by the Kissinger iso-conversion method is based on the equation [19]:

$$\ln\left[\frac{\ln\beta}{T^2}\right] = \ln\left[\frac{ZR}{E}\right] - \frac{E}{RT}. \quad (5)$$

The slope of the straight line plotted in coordinates  $\ln\left[\frac{\ln\beta}{T^2}\right]$  versus  $\left(\frac{1000}{T}\right)$  allows the activation energy  $E$  to be computed.

For the calculation kinetic parameters according to the Flynn-Wall-Ozawa model-free method was used the following equation, taking into account the Doyle's approximation [20]:

$$\ln\beta = \ln\left[\frac{Z \cdot E}{R \cdot g(\omega)}\right] - 5.331 - 1.052 \frac{E}{RT}. \quad (6)$$

("1000"/"T") along the slope of the straight line, the activation energy  $E$  was found.

A plot of  $\ln\left[\frac{g(\omega)}{T^2}\right]$  versus  $\left(\frac{1000}{T}\right)$  gives a straight line with the slope which allows the determination of the activation energy  $E$ .

A Coats-Redfern method, which refers to model-fitting methods, was also applied to determine the activation energy  $E$  [21]. The equation used in this method is of the form:

$$\ln\left[\frac{g(\omega)}{T^2}\right] = \ln\left[\frac{ZR}{\beta E}\left[1 - \frac{2RT}{E}\right]\right] - \frac{E}{RT}. \quad (7)$$

All calculations are made under the condition that the reaction order is  $n = 1$ .

### Results and Discussion

According to the result of the chromatography-mass spectrometric analysis, it was found that the obtained coal tar distillate comprised alkanes ( $C_{12}-C_{20}$ ), alkenes ( $C_{13}-C_{16}$ ), cycloalkanes ( $C_7-C_{11}$ ), alkylbenzenes ( $C_7-C_{11}$ ), bicyclic alkanes, phenyl-cycloalkanes, naphthalenes (alkylnaphthalenes), biphenyls (alkyl biphenyls), phenols and O-, N- and S-containing compounds. Table 1 shows the composition of distillate.

Table 1

The composition of the obtained coal tar distillate (&lt; 350 °C)

No	Compound	Area, %	No	Compound	Area, %
1	2	3	4	5	6
1	3-Methylpyridine	0.15	12	5-Decanone	0.20
2	1,3-Dimethylbenzene	0.11	13	2-Ethylphenol	5.4
3	3,5-Dimethylpyridine	0.21	14	1,3-Cyclopentanedione, 2-chloro-	0.19
4	Phenol	3.78	15	3,5-Dimethylphenol	3.32
5	3-Methylbenzyl mercaptan	0.21	16	Triquinacene	0.53
6	1-Methylpropyl benzene	0.14	17	2,6-Dimethylanisole	0.27
7	2-Cyclopenten-1-one, 2,3-dimethyl	0.27	18	3-Ethylphenol	1.90
8	1-Propynyl benzene	0.13	19	(3-Methyl-2-butenyl) benzene	0.22
9	2-Methylphenol	3.21	20	1,2-Benzenediol	0.52
10	4-Methylphenol	7.50	21	4,7-Dimethylbenzofuran	0.28
11	2,6-Dimethylpyridine	0.18	22	2-Propylphenol	0.43

Continuation of Table 1

1	2	3	4	5	6
23	2-Ethyl-6-methylphenol	1.03	55	1-Naphthalenol	1.15
24	2,3-Dimethylanisole	0.14	56	2(1H)-Quinolinone, 4,8-dimethyl	1.76
25	1-Ethyl-4-methoxy benzene	1.05	57	1,6,7-Trimethyl naphthalene	2.5
26	2,4-Dimethylanisole	1.84	58	1,4,6-Trimethyl naphthalene	0.84
27	1,2-Benzenediol, 3-methyl-	1.35	59	4,6,8-Trimethylazulene	1.47
28	3,4-Dimethylanisole	0.48	60	1-Heptadecene	1.35
29	Cyclohexane, 1,2,3-trimethyl-, (1 alpha., 2.beta., 3.alpha.)	0.38	61	Heptadecane	5.11
30	1H-Indene, 2,3-dihydro-4,7-dimethyl	0.27	62	1-methyl-7-(1-methylethyl) naphthalene	0.70
31	3,5-dimethyl octane	0.76	63	1-Naphthalenol, 2-methyl-	2
32	1,2-Benzenediol, 4-methyl	1.45	64	Ethanol, 2-(5-amino-6-chloropyrimidin-4-ylamino)-	1.32
33	2-Methyl naphthalene	3.08	65	1-Methyl-7-(1-methylethyl) naphthalene	0.43
34	1-(2-Hydroxy-5-methylphenyl) ethanone	0.40	66	Methyl diisopropylphosphoramordite	0.51
35	2-Methyl-5-(1-methylethyl) phenol	0.51	67	1,6-Dimethyl-4-(1-methylethyl) naphthalene	1.41
36	6,7-Dimethyl-1,2,3,4-tetrahydronaphthalene	0.54	68	9-Methoxyfluorene	0.53
37	1H-Inden-5-ol, 2,3-dihydro	0.86	69	1,4-Dihydro-2,5,8-tri methyl naphthalene	1.04
38	1,3-Benzenediol, 4-ethyl	0.71	70	1-Naphthol, 6,7-dimethyl-	1.19
39	6-Methyl-4-indanol	0.29	71	1-Naphthol, 5,7-dimethyl-	0.41
40	2-Ethyl-3-methoxypyrazine	1.61	72	N-Methoxy-2-carbomethoxy-2-carbeth oxyaziridine	0.33
41	1-(2,4-Dimethylphenyl) ethanone	0.51	73	N-Methyl-1-hydroxycarbazole	0.64
42	1,2,3-Trimethylindene	0.71	74	3-Methyl tetradecane	3
43	1,3-Cyclohexanedione, 5-isopropyl	0.45	75	Phenanthrene	0.35
44	1-(2,4-Dimethyl-furan-3-yl) ethanone	2.75	76	6-Methoxy-2-(1-buten-3-yl) naphthalene	0.32
45	1,2,3,4-Tetrahydro-1,1,6-trimethyl naphthalene	1.08	77	3,4-Dimethyl(1H)pyrrole, 2-[(3,4-d imethyl-[2H]-pyrrol-2-ylidene	0.24
46	2,7-Dimethyl naphthalene	1.28	78	Trifluoroacetoxy hexadecane	0.19
47	2-Allyl-4-methylphenol	0.32	79	Eicosane	2.45
48	2,3-Dimethyl naphthalene	3.19	80	7-Hydroxycadalene	0.20
49	1-(2,5-Dimethylphenyl) ethanone	2.06	81	1-Hexadecene	0.24
50	1-Pentadecene	0.70	82	Heneicosane	1.58
51	Pentadecane	1.57	83	Octadecyl trifluoroacetate	0.26
52	Acenaphthene	0.58	84	1-Methyl-7-(1-methylethyl) phenanthrene	0.41
53	3-Ethyl-1,2,4,5-tetramethyl benzene	0.90	85	11-Tricosene	0.16
54	2,3,6-Trimethyl naphthalene	0.64	86	Hentriacontane	2.3

SEM analysis (Fig. 1) showed that the nickel powder consists of nanoscale particles with a form close to spherical forming aggregates. The presence of small amount of oxygen and carbon were found by EDS (Fig. 1).

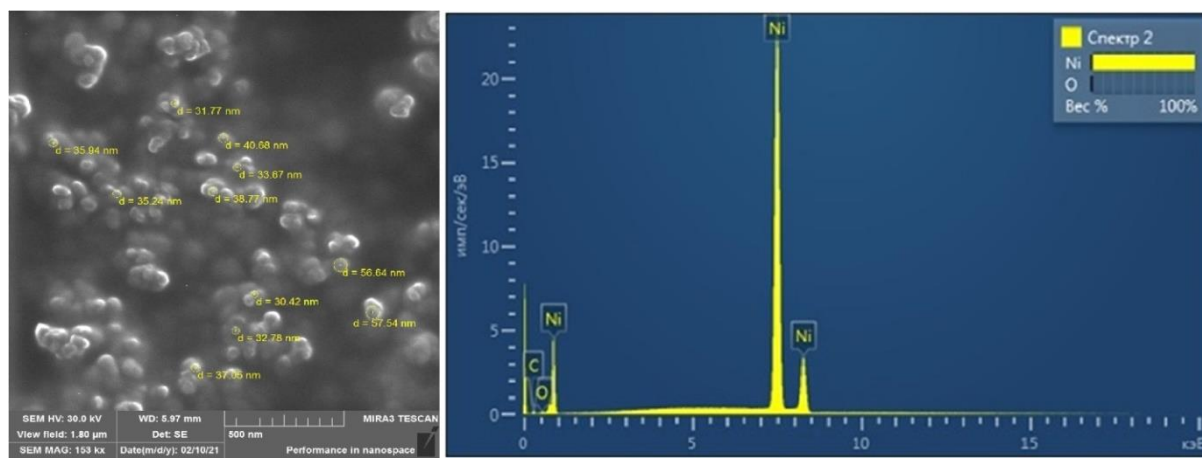


Figure 1. SEM image and EDS of nickel powder

On the XRD pattern (Fig. 2) basic peaks with the Miller indices (111), (200) and (220) were observed at the appropriate values of interplanar distances 2.034 Å, 1.762 Å and 1.246 Å. These parameters were in accordance with face-centered cubic structure. Calculation using the Equation (1) showed that medium crystallite size was approximately 34 nm.

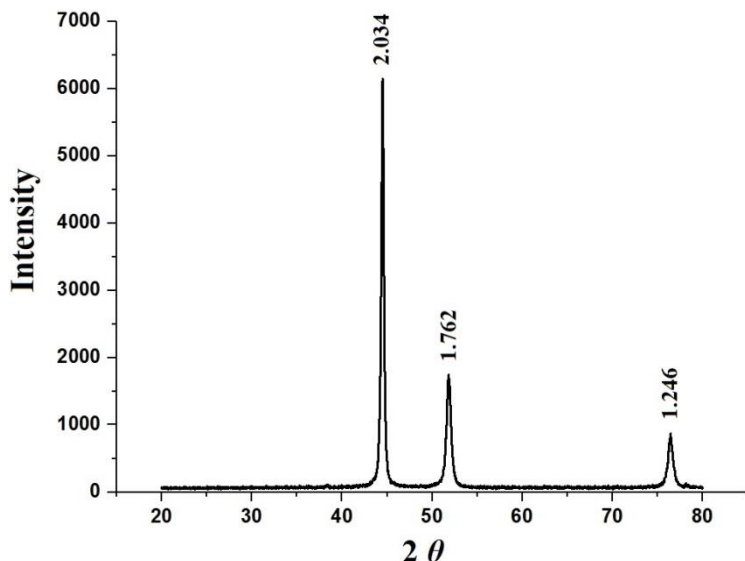
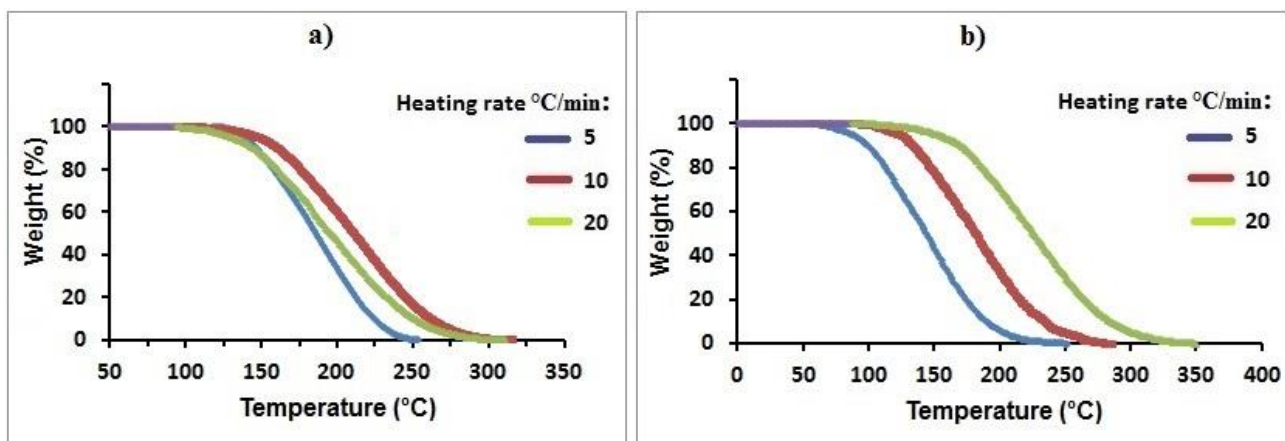


Figure 2. Diffraction pattern of the nickel powder

Figure 3 presents the effect of heating rate 5, 10 and 20 °C/min on weight loss (%).

The values of activation energies calculated by the Kissinger method showed that high correlation coefficients  $R^2 = 0.966\text{--}0.9915$  were received for the conversion  $\omega$  in the range of 20–60 % for thermal decomposition of primary coal tar distillate without a catalyst (Table 1).



*a* — without a catalyst; *b* — in the presence of nickel powder

Figure 3. The effect of heating rate 5, 10 and 20 °C/min on weight loss (%)

At a heating rate of 5 °C/min, a temperature shift of the start of degradation is observed from ~140 °C without a catalyst versus ~90 °C in the presence of nickel powder. The shift was from ~150 °C to ~125 °C for the heating rate 10 °C/min. Also, for the heating rate 20 °C/min the temperature of the start of degradation was ~125 °C without the catalyst and ~160 °C in the presence of nickel powder.

Figure 4 designates the plots obtained by the Kissinger method.

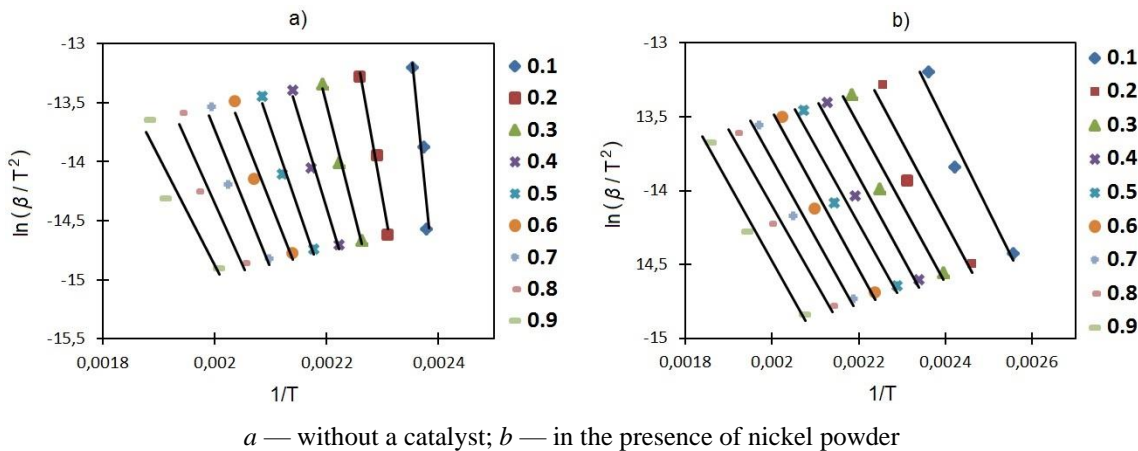


Figure 4. Kissinger approximation plots of thermal degradation of primary coal tar distillate

The average value of the activation energy  $E_a = 145.19 \text{ kJ/mol}$  was calculated from the activation energy values for conversion ( $\omega$ ) in the range 0.2–0.6 with correlation coefficients  $R^2 \geq 0.96$ .

Table 2

#### Calculation of activation energy at various conversions by the Kissinger method

Without a catalyst									
Conversion ( $\omega$ )	0.1	0.2	0.3	0.4	0.5	0.6	0.7	0.8	0.9
Correlation coefficient ( $R^2$ )	0.8481	0.9847	0.9915	0.9857	0.9832	0.963	0.9352	0.9177	0.8913
Activation energy ( $E_a, \text{ kJ/mol}$ )	392.98	220.04	158.42	131.9	114.97	100.62	96.77	87.07	76.62
In the presence of catalyst									
Conversion ( $\omega$ )	0.1	0.2	0.3	0.4	0.5	0.6	0.7	0.8	0.9
Correlation coefficient ( $R^2$ )	0.9403	0.9177	0.9359	0.9404	0.9514	0.9606	0.9682	0.9667	0.9762
Activation energy ( $E_a, \text{ kJ/mol}$ )	49.1	45.53	44.72	44.57	43.54	44.52	43.75	42.69	43.76

When calculating by the Kissinger method for the thermal decomposition of coal distillate with the addition of nanoscale nickel powder in a quantity of 1 % of distillate weight, the activation energies with correlation coefficients  $R^2 \leq 0.98$  were obtained for all the range of  $\omega = 0.1\text{--}0.9$  (Table 2). The average activation energy  $E_a = 43.65 \text{ kJ/mol}$  was calculated from the activation energies obtained in the range of  $\omega = 0.5\text{--}0.9$  with  $R^2 = 0.9514\text{--}0.9762$ .

Figure 5 illustrates the linear relationships obtained by the Flynn-Wall-Ozawa method.

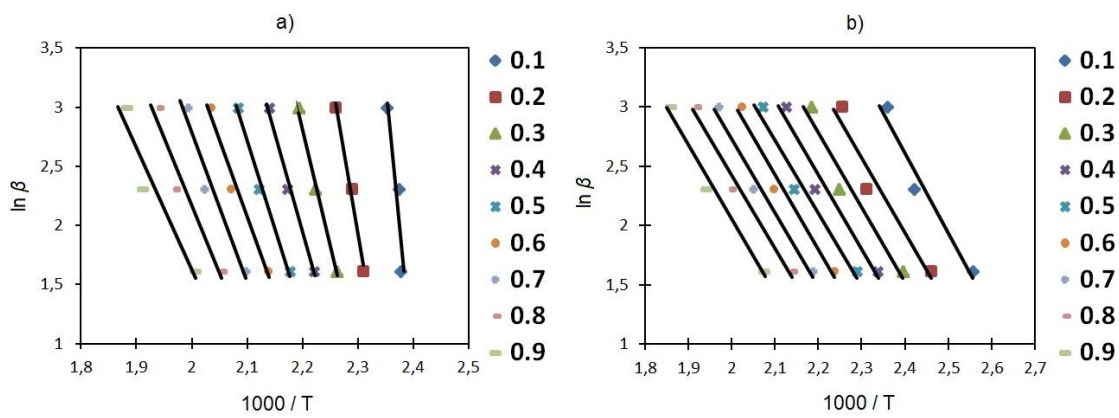


Figure 5. Linear relationships obtained by the Flynn-Wall-Ozawa method

The calculation of activation energies at various conversions by the FWO method (Table 3) showed that the highest correlation coefficients  $R^2$  were in the range of conversions  $\omega = 0.2\text{--}0.6$  for thermal decomposition of primary coal tar distillate without a catalyst. The average value of activation energy were calculated for  $\omega$  in the range 0.2–0.6 and accounted for  $E_a = 152.82 \text{ kJ/mol}$ .

Table 3

**Calculation of activation energy at various conversions by the FWO method**

Without a catalyst									
Conversion ( $\omega$ )	0.1	0.2	0.3	0.4	0.5	0.6	0.7	0.8	0.9
Correlation coefficient ( $R^2$ )	0.8527	0.9856	0.9922	0.9872	0.9852	0.9679	0.9441	0.9302	0.9098
Activation energy ( $E_a, \text{ kJ/mol}$ )	400	227.32	165.89	122.77	140.27	108.58	104.88	95.39	85.15
In the presence of catalyst									
Conversion ( $\omega$ )	0.1	0.2	0.3	0.4	0.5	0.6	0.7	0.8	0.9
Correlation coefficient ( $R^2$ )	0.9527	0.9364	0.9511	0.9549	0.9636	0.9705	0.9764	0.9756	0.9826
Activation energy ( $E_a, \text{ kJ/mol}$ )	55.85	52.57	51.97	52	51.15	51.31	51.74	50.88	51.2

Calculation by the FWO method for thermal decomposition of distillate with the addition of nickel powder (in a quantity of 1 % of distillate weight) showed that the values of activation energies were received at correlation coefficients  $R^2 < 0.99$  for all the range of conversion  $\omega = 0.1\text{--}0.9$ . The average activation energy  $E_a = 51.65 \text{ kJ/mol}$  was calculated from the activation energies obtained in the range  $\omega = 0.5\text{--}0.9$  with  $R^2 = 0.9636\text{--}0.9826$ .

Figure 6 demonstrates curves of thermal degradation of primary coal tar distillate in the presence of nickel powder constructed by the Coats-Redfern method.

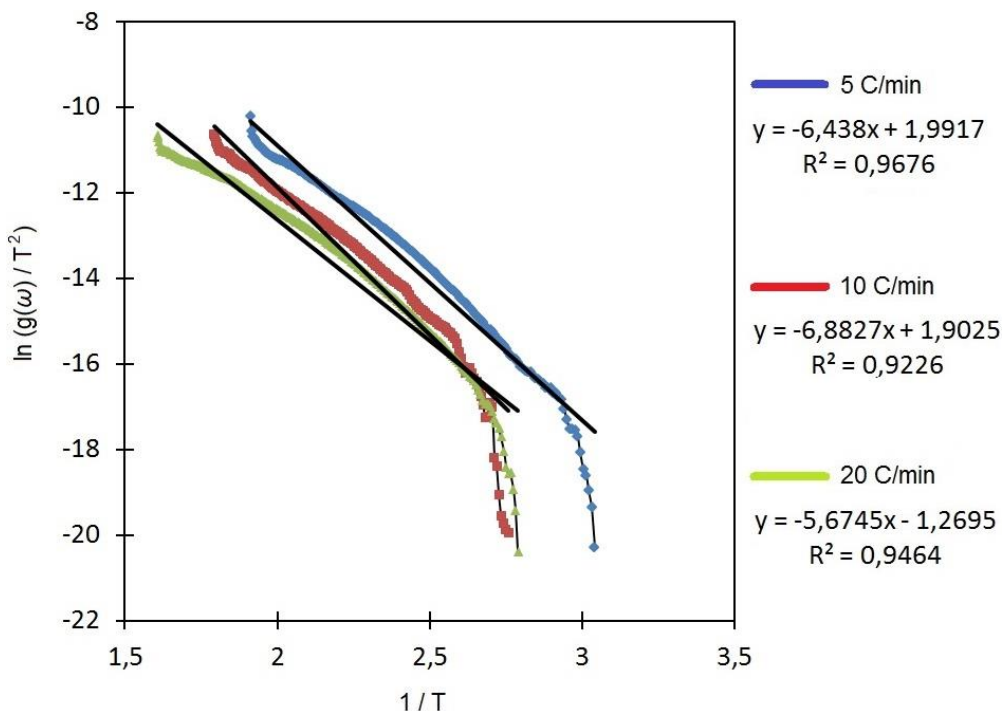


Figure 6. Curves of thermal degradation of primary coal tar distillate in the presence of nickel powder

The calculation of activation energies at different heating rates by the Coats-Redfern method is presented in Table 4.

Table 4

**Calculation of activation energies at different heating rates by the Coats-Redfern method**

Kinetic parameters	Without a catalyst			In the presence of nickel powder		
Heating rate (°C/min)	5	10	20	5	10	20
Activation energy ( $E_a$ , kJ/mol)	178.753	119.185	132.203	52.525	57.22	47.18
Correlation coefficient ( $R^2$ )	0.9926	0.9909	0.9935	0.9676	0.9226	0.9446
The average value of $E_a$ , kJ/mol	143.38			52.64		

According to the calculation received by the Coats-Redfern method for thermal degradation of primary coal tar distillate without a catalyst, the average activation energy was  $E_a = 143.38$  kJ/mol without a catalyst and was close to activation energy value obtained by the Kissinger method.

In the presence of nickel powder the activation energy was  $E_a = 52.64$  kJ/mol, which was close to activation energy value obtained by the FWO method.

*Conclusions*

The results of this study revealed that in the process of thermal degradation of primary coal tar distillate (<350 °C) the values of activation energy calculated by the model-free Kissinger and Flynn-Wall-Ozawa methods are consistent with the model-fitting Coats-Redfern method. The differential between obtained values is insignificant. The calculation of the activation energy with high correlation coefficients is provided by the Kissinger and FWO methods for the process of thermal degradation of primary coal tar distillate (<350 °C) without a catalyst.

The Coats-Redfern method is also suitable for calculating the activation energy in the presence of nickel nanopowder, because obtained dependences are close to linear and have the high correlation coefficients. It was found that the addition of nanoscale nickel powder in a quantity of 1 % of distillate weight the activation energy reduces by approximately 3 times.

**References**

- 1 Zhang H. Selective hydrogenation of aromatics in coal-derived liquids over novel NiW and NiMo carbide catalysts / H. Zhang, G. Chen, L. Bai, N. Chang, Y. Wang // Fuel. — 2019. — Vol. 244. — P. 359–365. <https://doi.org/10.1016/j.fuel.2019.02.015>
- 2 Lei Z. Gas-Modified Pyrolysis Coke for in Situ Catalytic Cracking of Coal Tar / Lei, S. Hao S., Z. Lei, J. Yang // ACS Omega. — 2020. — Vol. 5. — P. 14911–14923. <https://doi.org/10.1021/acsomega.0c00055>
- 3 Baig N. Nanomaterials: a review of synthesis methods, properties, recent progress, and challenges / N. Baig, I. Kammakakam, W. Falathabe // Materials Advances. — 2020. — Vol. 2. — P. 1821–1871. <https://doi.org/10.1039/DOMA00807A>
- 4 Khalil M. Advanced nanomaterials in oil and gas industry: Design, application and challenges / M. Khalil, B.M. Jan, C.W. Tong, M.A. Berawi // Applied energy. — 2017. — Vol. 191. — P. 287–310. <https://doi.org/10.1016/j.apenergy.2017.01.074>
- 5 Suwaid M. In-situ catalytic upgrading of heavy oil using oil-soluble transition metal-based catalysts / M. Suwaid, V.A. Varfolomeev, A.A. Al-muntaser, C. Yuan, V.I. Starshinova, A. Zinnatullin, F.G. Vagizov, I.Z. Rakhmatullin, D.A. Emelian, A.E. Chemodanov // Fuel. — 2020. — Vol. 281. — No. 118753. <https://doi.org/10.1016/j.fuel.2020.118753>
- 6 Khoshooei M.A. Activity assessment of NiMo bimetallic nanocatalyst in presence and absence of steam in in-situ upgrading technology (ISUT) / M.A. Khoshooei, S.M. Elahi, L. Carbognani, C.E. Scott // Fuel. — 2021. — Vol. 288. — No. 119664. <https://doi.org/10.1016/j.fuel.2020.119664>
- 7 Wang W. Bifunctional catalysts for the hydroisomerization of n-alkanes: the effects of metal–acid balance and textural structure / W. Wang, C.J. Liu, W. Wu // Catalysis Science & Technology. — 2019. — Vol. 9. — P. 4162–4187. <https://doi.org/10.1039/C9CY00499H>
- 8 Gang Y. Hydroprocessing of low-temperature coal tar to produce jet fuel / Y. Gang, X. Zhang, X. Lei, H. Guo, W. Li, D. Li // RSC Advances. — 2018. — Vol. 8, Issue 42. — P. 23663–23670. <https://doi.org/10.1039/C8RA04531C>
- 9 Kan T. Production of Gasoline and Diesel from Coal Tar via Its Catalytic Hydrogenation in Serial Fixed Beds / T. Kan, X. Sun, H. Wang, C. Li, U. Muhammad // Energy & Fuels. — 2012. — Vol. 26, Issue 6. — P. 3604–3611. <https://doi.org/10.1021/EF3004398>
- 10 Qi S.C. A highly active Ni/ZSM-5 catalyst for complete hydrogenation of polymethylbenzenes / S.C. Qi, X.Y. Wei, Z.M. Zong, J.I. Hayashi, X.H. Yuan, L.B. Sun L.B. // ChemCatChem. — 2013. — Vol. — 5, Issue 12. — P. 3543–3547. <https://doi.org/10.1002/cctc.201300547>

11 Малолетнев А.С. Гидрооблагораживание каменноугольной смолы в присутствии наногетерогенных никельсульфидных катализаторов / А.С. Малолетнев, Ж.К. Каирбеков, Н.Т. Смагулова // Кокс и химия. — 2020. — № 5. — С. 253–256. <https://doi.org/10.3103/S1068364X20050038>

12 Байкенов М.И. Влияние новых каталитических систем на процесс гидрогенизации антрацена / М.И. Байкенов, Г.Г. Байкенова, А.С. Исадаев, А.Б. Татеева, Ж.С. Ахметкаrimova, А. Тусипхан, А.Ж. Матаева, К.К. Есенбаева // Химия твердого топлива. — 2015. — № 3. — С. 22–27. <https://doi.org/10.7868/S0023117715030032>

13 Baikenov M.I. Hydrogenation of polyaromatic compounds over NiCo/chrysotile catalyst / M.I. Baikenov, D.E. Aitbekova, N.Zh. Balpanova, A. Tusipkhan, G.G. Baikenova, Y.A. Aubakirov, A.R. Brodskiy, F. Ma, D.K. Makenov // Bulletin of the University of Karaganda — Chemistry. — 2021. — Vol. 103, No. 3. — P. 74–82. <https://doi.org/10.31489/2021Ch3/74-82>

14 Balpanova N.Zh. Thermokinetic parameters of the primary coal tars destruction in the presence of catalysts and polymeric materials / N.Zh. Balpanova, M.I. Baikenov, A.M. Gyulmaliev, Z.B. Absat, Zh. Batkhan, F. Ma, K. Su, S.V. Kim, G.G. Baikenova, D.E. Aitbekova, A. Tusipkhan // Bulletin of the University of Karaganda — Chemistry. — 2021. — Vol. 102, No. 2. — P. 86–95. <https://doi.org/10.31489/2021Ch2/86-95>

15 Ким С.В. Каталитические свойства ультрадисперсного порошка никеля при гидрогенизации антрацена и фенантрена / С.В. Ким, К.С. Ибишев, М.И. Байкенов, А. Тусупхан, В.П. Григорьева, А.М. Гюлмалиев // Химия твердого топлива. — 2022. — № 1. — С. 36–42. <https://doi.org/10.31857/s002311772010029>

16 Vyazovkin S. ICTAC Kinetics Committee recommendations for performing kinetic computations on thermal analysis data / S. Vyazovkin, A.K. Burnham, J.M. Criado, L.A. Pérez-Maqueda, C. Popescu, N. Sbirrazzuoli // Thermochimica Acta. — 2011. — Vol. 520. — P. 1–19. <https://doi.org/10.1016/j.tca.2011.03.034>

17 Loy A. Thermogravimetric kinetic modelling of 1 in-situ catalytic pyrolytic conversion of rice husk to bioenergy using rice hull ash catalyst / A. Loy, D. Gan, S. Yusup, B. Chin, M.K. Lam, M. Shahbaz, P. Unrean, M.N. Acda, E. Rianawati // Bioresource Technology. — 2018. — Vol. 261. — P. 213–222. <https://doi.org/10.1016/j.biortech.2018.04.020>

18 Heydari M. Kinetic Study and Thermal Decomposition Behavior of Lignite Coal / M. Heydari, M. Rahman, R. Gupta // International Journal of Chemical Engineering. — 2015. — Article ID 481739. <https://doi.org/10.1155/2015/481739>

19 Yao Z. Comparative study on the pyrolysis kinetics of polyurethane foam from waste refrigerators. / Z. Yao, S. Yu, W. Su, W. Wu, J. Tang, W. Qi // Waste Management & Research. — 2019. — Vol. 38, Issue 3. — P. 271–278. <https://doi.org/10.1177/0734242X19877682>

20 Balart R. Kinetic analysis of the thermal degradation of recycled acrylonitrile-butadiene-styrene by non-isothermal thermogravimetry / R. Balart, D. Garcia-Sanoguera, L. Quiles-Carrillo, N. Montanes, G. Torres-Giner // Polymers. — 2019. — Vol. 11, Issue 2. — No. 281. <https://doi.org/10.3390/polym11020281>

21 Козлов А.Н. Кинетический анализ термохимической конверсии твердых топлив / А.Н. Козлов, Д.А. Свищева, Д.И. Худякова, А.Ф. Рыжков // Химия твердого топлива. — 2017. — № 4. — С. 12–21. <https://doi.org/10.7868/S0023117717040028>

С.В. Ким, М.И. Байкенов, К.С. Ибишев,  
М.Г. Мейрамов, Фен Юн Ма, Т.О. Хамитова

## Тасқомір шайыры дистиллятының термиялық ыдырауына никель наноұнтағының әсері

Тасқомір шайыры дистиллятының термиялық ыдырау процесіне никель наноұнтағының әсер ету заңдылықтары Киссинджер, Флинн-Уолл-Озаваның динамикалық модельсіз әдістерін және Коутс-Редфернің модельді әдісін қолдана отырып анықтады. Қайнау температурасы  $<350^{\circ}\text{C}$  болатын тасқомір шайырының дистилляты Шубаркөл кен орнының біріншілік тасқомір шайырын қарапайым айдау арқылы алынды. Катализатор ретінде қолданылған никель ұнтағы тасқомір шайырының дистиллятының термиялық ыдырау процесі инергіті газ ортасында 5, 10 және  $20^{\circ}\text{C}/\text{мин}$  қыздыру жылдамдықтарымен жүргізілді. Никель ұнтағы электролиз процесіне тұрақты токта жоғары вольтты разрядпен әсер еткен кезде алынды. Рентгендік фазалық анализ (РФА) алынған никель ұнтағы центрліктерді текше құрылымды екенін көрсетті, ал Шеррер тендеуімен есептелген кристаллліттердің орташа өлшемі шамамен 34 нм құрады. Активителу энергиясын есептеу термогравиметриялық мәліметтерді өңдеу арқылы жүргізілді. Киссинджер әдісі бойынша есептеу активителу энергиясының мәні 145,19 кДж/моль-ден 43,65 кДж/моль-ге дейін төмендейтін көрсетті, Флинн-Уолл-Озава (FWO) әдісі бойынша активителу энергиясының мәні 152,82 кДж/моль-ден 51,65 кДж/моль-ге дейін төмендейтін анықталды және Коутс-Редферн модельдік әдісіне сәйкес активителу энергиясының мәні 143,38 кДж/моль-ден 52,64 кДж/моль-ге дейін төмендейді. Алынған корреляция коэффициенттерінің жоғары мәндері бұл әдістердің колданылу мүмкіншілігін аныктайды.

*Кітт сөздер:* термиялық деструкция, никель, наноұнтақ, тасқомір шайыры, дистиллят, кристаллит, термогравиметриялық анализ, активителу энергиясы.

С.В. Ким, М.И. Байкенов, К.С. Ибишев,  
М.Г. Мейрамов, Фен Юн Ма, Т.О. Хамитова

## Влияние нанопорошка никеля на термическое разложение дистиллята каменноугольной смолы

Закономерности влияния нанопорошка никеля на процесс термического разложения дистиллята каменноугольной смолы были определены с использованием динамических безмодельных методов Киссинджера, Флинна–Уолла–Озавы и модельного метода Коутса–Редферна. Дистиллят каменноугольной смолы с температурой кипения < 350 °C был получен простой перегонкой первичной каменноугольной смолы с месторождения «Шубарколь». В качестве катализатора использовали наноразмерный порошок никеля, который добавляли в дистиллят каменноугольной смолы в количестве 1 % от массы дистиллята и затем проводили процесс термической деструкции дистиллята каменноугольной смолы при скоростях нагрева 5, 10 и 20 °C/мин в среде инертного газа. Порошок никеля был получен при воздействии высоковольтного разряда на процесс электролиза на постоянном токе. Проведенный рентгенофазовый анализ показал, что полученный порошок никеля имеет гранецентрированную кубическую структуру, а средний размер кристаллитов, рассчитанный по уравнению Шеррера, составил примерно 34 нм. Расчеты энергии активации проводились с помощью обработки термогравиметрических данных. Расчет по методу Киссинджера показал, что значение энергии активации уменьшается с 145,19 кДж/моль до 43,65 кДж/моль, по методу Флинна–Уолла–Озавы установлено, что значение энергии активации уменьшается с 152,82 кДж/моль до 51,65 кДж/моль, и согласно модельному методу Коутса–Редферна значение энергии активации уменьшается со 143,38 кДж/моль до 52,64 кДж/моль. Применимость данных методов обеспечивается полученными высокими значениями коэффициентов корреляции.

**Ключевые слова:** термическая деструкция, никель, нанопорошок, каменноугольная смола, дистиллят, кристаллит, термогравиметрический анализ, энергия активации.

## References

- 1 Zhang, H., Chen, G., Bai, L., Chang, N., & Wang, Y. (2019). Selective hydrogenation of aromatics in coal-derived liquids over novel NiW and NiMo carbide catalysts. *Fuel*, 244, 359–365. <https://doi.org/10.1016/j.fuel.2019.02.015>
- 2 Lei, Z., Hao, S., Lei, Z., & Yang, J. (2020). Gas-Modified Pyrolysis Coke for In Situ Catalytic Cracking of Coal Tar. *ACS Omega*, 5, 14911–14923. <https://doi.org/10.1021/acsomega.0c00055>
- 3 Baig, N., Kammakakam, I., & Falathabe, W. (2021). Nanomaterials: a review of synthesis methods, properties, recent progress, and challenges. *Materials Advances*, 2, 1821–1871. <https://doi.org/10.1039/D0MA00807A>
- 4 Khalil, M., Jan, B.M., Tong, C.W., & Berawi, M.A. (2017). Advanced nanomaterials in oil and gas industry: Design, application and challenges. *Applied energy*, 191, 287–310. <https://doi.org/10.1016/j.apenergy.2017.01.074>
- 5 Suwaid, M., Varfolomeev, V.A., Al-muntaser, A.A., Yuan, C., Starshinova, V.I., Zinnatullin, A., Vagizov, F.G., Rakhmatullin, I.Z., Emelian, D.A., & Chemodanov, A.E. (2020). In-situ catalytic upgrading of heavy oil using oil-soluble transition metal-based catalysts. *Fuel*, 281, 118753. <https://doi.org/10.1016/j.fuel.2020.118753>
- 6 Khoshooei, M.A., Elahi, S.M., Carbognani, L., & Scott, C.E. (2021). Activity assessment of NiMo bimetallic nanocatalyst in presence and absence of steam in in-situ upgrading technology (ISUT) *Fuel*, 288, 119664. <https://doi.org/10.1016/j.fuel.2020.119664>
- 7 Wang, W., Liu, C.J., & Wu, W. (2019). Bifunctional catalysts for the hydroisomerization of *n*-alkanes: the effects of metal–acid balance and textural structure. *Catalysis Science & Technology*, 9, 4162–4187. <https://doi.org/10.1039/C9CY00499H>
- 8 Gang, Y., Zhang, X., Lei, X., Guo, H., Li, W., & Li, D. (2018). Hydroprocessing of low-temperature coal tar to produce jet fuel. *RSC Advances*, 8(42), 23663–23670. <https://doi.org/10.1039/C8RA04531C>
- 9 Kan T., Sun X., Wang H., Li, C., & Muhammad, U. (2012). Production of Gasoline and Diesel from Coal Tar via Its Catalytic Hydrogenation in Serial Fixed Beds. *Energy & Fuels*, 26(6), 3604–3611. <https://doi.org/10.1021/EF3004398>
- 10 Qi, S.C., Wei, X.Y., Zong, Z.M., Hayashi, J.I., Yuan, X.H., & Sun, L.B. (2013). A highly active Ni/ZSM-5 catalyst for complete hydrogenation of polymethylbenzenes. *ChemCatChem*, 5(12), 3543–3547. <https://doi.org/10.1002/cctc.201300547>
- 11 Maloletnev, A.S., Kairbekov Zh.K., & Smagulova, N.T. (2020). Gidrooblagorazhivanie kamennougolnoi smoly v prisutstvii nanogeterogenykh nikelsukfidnykh katalizatorov [Refining of coal tar by hydrogenation in the presence of nanoheterogeneous nickel sulfide catalyst]. *Koks i khimiia — Coke and Chemistry*, 63(5), 253–256. <https://doi.org/10.3103/S1068364X20050038>
- 12 Baikenov, M.I., Baikenova, G.G., Isabaev, A.S. et al. Effect of new catalytic systems on the process of anthracene hydrogenation. *Solid Fuel Chem.* 49, 150–155 (2015). <https://doi.org/10.3103/S0361521915030039>
- 13 Baikenov, M.I., Aitbekova, D.E., Balpanova, N.Zh., Tusipkhan, A., Baikenova, G.G., Aubakirov, Y.A., Brodskiy, A.R., Ma, F., & Makenov, D.K. (2021). Hydrogenation of polycyclic aromatic compounds over NiCo/chrysotile catalyst. *Bulletin of the University of Karaganda — Chemistry*, 103(3), 74–82. <https://doi.org/10.31489/2021Ch3/74-82>

- 14 Balpanova, N.Zh., Baikenov, M.I., Gyulmaliev, A.M., Absat, Z.B., Batkhan, Zh., Ma, F., Su, K., Kim, S.V., Baikenova, G.G., Aitbekova, D.E., & Tusipkhan, A. (2021). Thermokinetic parameters of the primary coal tars destruction in the presence of catalysts and polymeric materials. *Bulletin of the University of Karaganda — Chemistry*, 102(2), 86–95. <https://doi.org/10.31489/2021Ch2/86-95>
- 15 Kim, S.V., Ibishev, K.S., Baikenov, M.I. et al. Catalytic Properties of Ultrafine Nickel Powder in the Hydrogenation of Anthracene and Phenanthrene. *Solid Fuel Chem.* 56, 53–58 (2022). <https://doi.org/10.3103/S0361521922010025>
- 16 Vyazovkin, S., Burnham, A.K., Criado, J.M., Pérez-Maqueda, L.A., Popescu, C., & Sbirrazzuoli, N. (2011). ICTAC Kinetics Committee recommendations for performing kinetic computations on thermal analysis data. *Thermochimica Acta*, 520, 1–19. <https://doi.org/10.1016/j.tca.2011.03.034>
- 17 Loy, A., Gan, D., Yusup, S., Chin, B., Lam, M.K., Shahbaz, M., Unrean, P., Acda, M.N., & Rianawati, E. (2018). Thermo-gravimetric kinetic modelling of 1 in-situ catalytic pyrolytic conversion of rice husk to bioenergy using rice hull ash catalyst. *Bioresource Technology*, 261, 213–222. <https://doi.org/10.1016/j.biortech.2018.04.020>
- 18 Heydari, M., Rahman, M., & Gupta, R. (2015). Kinetic Study and Thermal Decomposition Behavior of Lignite Coal. *International Journal of Chemical Engineering*. <https://doi.org/10.1155/2015/481739>
- 19 Yao, Z., Yu, S., Su, W., Wu, W., Tang, J., & Qi, W. (2019). Comparative study on the pyrolysis kinetics of polyurethane foam from waste refrigerators. *Waste Management & Research*, 38(3), 271–278. <https://doi.org/10.1177/0734242X19877682>
- 20 Balart, R., Garcia-Sanoguera, D., Quiles-Carrillo, L., Montanes, N., & Torres-Giner, G. (2019). Kinetic analysis of the thermal degradation of recycled acrylonitrile-butadiene-styrene by non-isothermal thermogravimetry. *Polymers*, 11(2), 281, 1–23. <https://doi.org/10.3390/polym11020281>
- 21 Kozlov, A.N., Svishchev, D.A., Khudiakova, G.I. et al. (2017) A kinetic analysis of the thermochemical conversion of solid fuels (A review). *Solid Fuel Chem.* 51, 205–213. <https://doi.org/10.3103/S0361521917040061>

#### Information about authors<sup>\*</sup>

**Kim, Sergey Valerievich** (corresponding author) — Doctoral student, Karagandy University of the name of academician E.A. Buketov, Universitetskaya street, 28, 100024, Karaganda, Kazakhstan; Research Engineer, Zh. Abishev Chemical-Metallurgical Institute, Karaganda, Ermekov street, 63, 100009, Kazakhstan; e-mail: [vanquishV8@mail.ru](mailto:vanquishV8@mail.ru); <https://orcid.org/0000-0002-6044-9438>;

**Baikenov, Murzabek Ispolovich** — Doctor of Chemical Sciences, Professor, Karagandy University of the name of academician E.A. Buketov, Universitetskaya street, 28, 100024, Karaganda, Kazakhstan; e-mail: [murzabek\\_b@mail.ru](mailto:murzabek_b@mail.ru); <https://orcid.org/0000-0002-8703-0397>;

**Ibishev, Kanat Sansyzbaevich** — Candidate of Chemical Sciences, Leading Researcher, Zh. Abishev Chemical-Metallurgical Institute, Karaganda, Ermekov street, 63, 100009, Kazakhstan; e-mail: [ikan-at2014@mail.ru](mailto:ikan-at2014@mail.ru); <https://orcid.org/0000-0001-7622-2791>;

**Meiramov, Mazhit Gabdullovich** — Candidate of Chemical Sciences, Senior Researcher, Institute of Organic Synthesis and Coal Chemistry of the Republic of Kazakhstan, Karaganda, Alihanova street, 1, 100008, Kazakhstan; e-mail: [majit\\_m@mail.ru](mailto:majit_m@mail.ru); <https://orcid.org/0000-0003-2498-6516>;

**Ma, Fengyun** — PhD, Professor, Xinjiang University, Urumqi, Nan Min Lu street, 666, Xinjiang Uyghur Autonomous Region (XUAR) People's Republic of China (PCR); e-mail: [ma\\_fy@126.com](mailto:ma_fy@126.com);

**Khamitova, Tolkyn Ondirisovna** — PhD, Agronomic Faculty, S. Seifullin Kazakh Agro Technical University, Nur-Sultan, Zhenis avenue, 62, 010011, Kazakhstan; e-mail: [khamitova.t@inbox.ru](mailto:khamitova.t@inbox.ru); <https://orcid.org/0000-0002-4691-3732>

\*The author's name is presented in the order: *Last Name, First and Middle Names*